This is an open access article published under an ACS AuthorChoice License, which permits copying and redistribution of the article or any adaptations for non-commercial purposes.

ACS central science

http://pubs.acs.org/journal/acscii

Research Article

What Is Special about Aromatic−Aromatic Interactions? Significant Attraction at Large Horizontal Displacement

Dragan B. Ninković, Jelena P. Blagojević Filipović, Michael B. Hall,* Edward N. Brothers, and Snežana D. Zarić*

Cite This: ACS Cent. Sci. 2020, 6, 420−425

Read Online

ACCESS | Metrics & More | Article Recommendations | Supporting Information

ABSTRACT: High-level *ab initio* calculations show that the most stable stacking for benzene−cyclohexane is 17% stronger than that for benzene−benzene. However, as these systems are displaced horizontally the benzene−benzene attraction retains its strength. At a displacement of 5.0 Å, the benzene−benzene attraction is still ∼70% of its maximum strength, while benzene−cyclohexane attraction has fallen to ∼40% of its maximum strength. Alternatively, the radius of attraction (>2.0 kcal/mol) for benzene−benzene is 250% larger than that for benzene−cyclohexane. Thus, at relatively large distances aromatic rings can recognize each other, a phenomenon that helps explain their importance in protein folding and supramolecular structures.

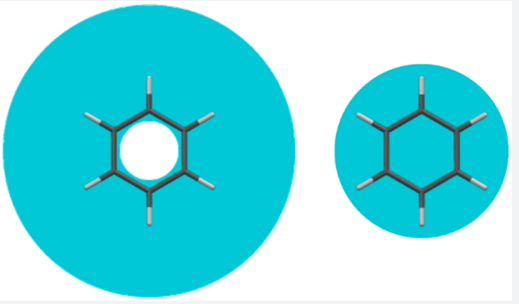

INTRODUCTION

Aromatic−aromatic interactions[1−49] have been invoked as key features of a number of molecular phenomena: protein folding,[34−37] crystal engineering,[38−41] catalysis,[42−46] and drug design.[1,47−49] Explanations have suggested that there is something special about these interactions.[15,17,20,21] However, it has been clearly demonstrated that the aromaticity is not the key as nonaromatic, planar 6π electron systems have stacking energies similar to those of benzene.[17] Here, we will use the term aromatic−aromatic interactions as most observations fall into that category, but our conclusions will apply in other cases.

Unexpectedly, the calculated interaction energies for the stacking of cyclohexane dimers are nearly as large as that for benzene dimers.[18] Furthermore, the stacking interaction between benzene and cyclohexane is somewhat stronger than either homodimer.[19] In all of these interactions, electrostatic and dispersion play important roles, but dispersion is larger in benzene dimer.[18,20] As the molecules become larger, more favorable dispersion and less repulsion in large aromatic systems, with more than 10−15 carbon atoms, contributes to stronger aromatic stacking interactions in comparison to aliphatic.[15,21]

Numerous computational studies of the interaction energy between two benzene molecules[22−30] have established that the most stable benzene dimer has the tilted T-shape (edge-to-face), with a CCSD(T)/CBS interaction energy of −2.84 kcal/mol,[29] while the most stable stacking benzene−benzene interaction has a geometry with a parallel displacement (offset) of 1.5 Å, and an interaction energy of −2.79 kcal/mol.[30] Recent work has shown that substantial interaction energies of around −2.0 kcal/mol are predicted for larger offsets of 4.0−5.0 Å.[30] Furthermore, statistical analysis of the data from the Cambridge Structural Database (CSD) showed that the preferred stacking (parallel) benzene−benzene interactions in crystal structures are at large horizontal displacements (3.5−5.0 Å), and not at the 1.5 Å, where the energy minimum lies in the gas-phase dimer. Similar large displacements are also found for interactions between aromatic rings of phenylalanine in proteins,[31] and pyridine−pyridine interactions in crystal structures from the CSD.[32]

In this work, we compared potential energy curves for stacking benzene−benzene vs stacking benzene−cyclohexene interactions, including large horizontal displacements. We also analyzed the nature of these interactions by performing SAPT analyses.

Calculations at high level, including the coupled-cluster/complete-basis-set limit, CCSD(T)/CBS, show that benzene−benzene dimers have a much large radius of attraction compare to benzene−cyclohexane dimers (Figure 1) in spite of the benzene−cyclohexane dimers having a larger attraction energy at their corresponding minimum energy structures. Details of these calculations and a SAPT analysis of contributing energy components are described in this paper.

RESULTS AND DISCUSSION

Important insight about the specificity of aromatic−aromatic interactions can be obtained by comparing the calculated

Received: January 2, 2020
Published: March 2, 2020

Downloaded via NATL LBRY OF SERBIA on May 26, 2020 at 09:01:51 (UTC).
See https://pubs.acs.org/sharingguidelines for options on how to legitimately share published articles.

© 2020 American Chemical Society

https://dx.doi.org/10.1021/acscentsci.0c00005
ACS Cent. Sci. 2020, 6, 420−425

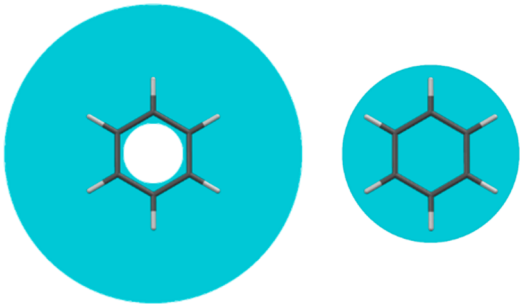

Figure 1. Areas in which attractive interaction energy is larger than −2.0 kcal/mol for benzene−benzene (left) and benzene−cyclohexane (right).

potential energy curves for cyclohexane−benzene,[19] and benzene−benzene stacking interactions,[30] following the geometric parameters shown in Figure 2.

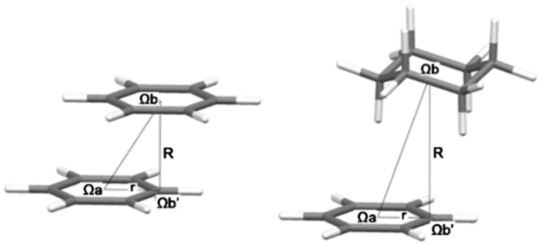

Figure 2. Geometric parameters used in calculations of benzene−benzene and cyclohexane−benzene interactions. Ω_a and Ω_b denote benzene or cyclohexane ring centers. R denotes distance between parallel mean planes of the rings, while Ω_b' are benzene and cyclohexane ring centers projections onto the benzene rings planes; r denotes displacement of the second ring projection on the benzene.

Accurate potential energy curves were calculated by high-level quantum chemical methods,[19,30] which are in good agreement with CCSD(T)/CBS,[33,50] with Gaussian09[51] (version D.01, the details of the calculations are given in the SI).

The data in Figure 3 show the variation of the average interaction energy as one ring is displaced from the other ring (r) and maintained at the minimum distance apart (R). The average is done with respect to three possible rotational orientations of the rings and displacements in both the left and

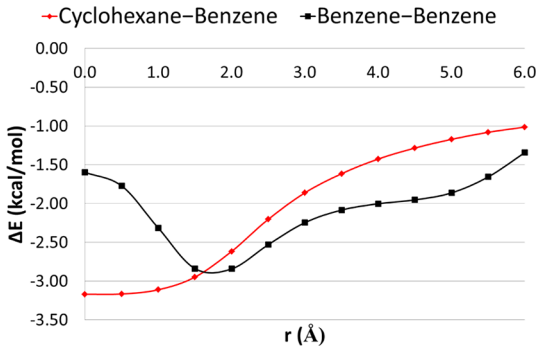

Figure 3. Calculated interaction energies averaged over the three possible orientations and two directions for cyclohexane−benzene[19] and benzene−benzene[30] (Figures S1 and S2) plotted as a function of the displacement (r) (Figure 1).

right direction (see Figures S1 and S2 for details of the orientations and all six interaction energy curves). The largest difference in average energies is at small offsets (<1.0 Å), where the cyclohexane−benzene dimer is significantly more stable than the benzene−benzene dimer (Figure 3, Tables 1 and 2).

Table 1. Results of SAPT Analysis and CCSD(T)/CBS Calculations for Benzene−Benzene Interactions at Several Offset Values (Figure 2)[a]

	offset (r)			
	r = 0.0	r = 1.5	r = 4.0	r = 5.0
normal distance (R)	3.90	3.50	3.20	2.67
electrostatics	0.09	−1.50	−1.30	−1.31
exchange	3.28	6.58	3.10	2.67
induction	−0.22	−0.70	−0.35	−0.30
dispersion	−5.00	−7.21	−3.47	−2.95
net dispersion[b]	−1.72	−0.62	−0.38	−0.28
total SAPT2+3	−1.85	−2.83	−2.03	−1.89
CCSD(T)/CBS	−1.75	−2.78	−2.02	−1.85
% of the most stable interaction[c]	63	100	72	69

[a]Offset and normal distance values are given in Å. All interaction energies and energy components are average for the three potential curves (Tables S1−S3) and given in kcal/mol. [b]Net dispersion is sum of dispersion and exchange terms. [c]The most stable interaction is for minimum at Abb curve with energy of −2.79 kcal/mol (Figure S2).

Table 2. Results of SAPT Analysis and CCSD(T)/CBS Calculations for Cyclohexane−Benzene Interactions at Several Offset Values (Figure 2)[a]

	offset (r)			
	r = 0.0	r = 1.5	r = 4.0	r = 5.0
normal distance (R)	4.20	4.00	3.65	3.03
electrostatics	−1.75	−1.92	−0.65	−0.55
exchange	4.61	5.36	2.30	2.05
induction	−0.57	−0.59	−0.25	−0.21
dispersion	−5.49	−5.89	−2.99	−2.66
net dispersion[b]	−0.88	−0.54	−0.69	−0.61
total SAPT2+3	−3.20	−3.02	−1.59	−1.38
CCSD(T)/CBS	−3.15	−2.88	−1.55	−1.35
% of the most stable interaction[c]	96	88	47	41

[a]Offset and normal distance values are given in Å. All interaction energies and energy components are average for the three potential curves (Tables S4−S6) and given in kcal/mol. [b]Net dispersion is sum of dispersion and exchange terms. [c]The most stable interaction is for minimum at Abc curve with energy of −3.27 kcal/mol (Figure S2).

and 2). At offset 0.0 Å (sandwich or face-to-face geometry) the CCSD(T)/CBS average interaction energy for cyclohexane−benzene is −3.15 kcal/mol, while the average benzene−benzene interaction energy is −1.75 kcal/mol. Benzene−benzene has its strongest interaction energy, −2.78 kcal/mol, at an offset about 1.5 Å, where the average cyclohexane−benzene interaction energy is nearly the same value.

An important difference between the average cyclohexane−benzene and benzene−benzene stacking energies also occurs at large offsets, where that for benzene−benzene is stronger. At large offsets (4.0−5.0 Å) the cyclohexane−benzene energies are only 41−47% of their minimum energy, while the

https://dx.doi.org/10.1021/acscentsci.0c00005
ACS Cent. Sci. 2020, 6, 420−425

benzene−benzene energies are 69−72% of their minimum energy (Tables 1 and 2).

In addition to relatively strong interactions (Figure 3, Table 1) the interactions at large offsets leave faces of benzene molecules available for additional interactions with surrounding species in supramolecular structures. One example is shown in Figure 4a where every benzene ring has additional

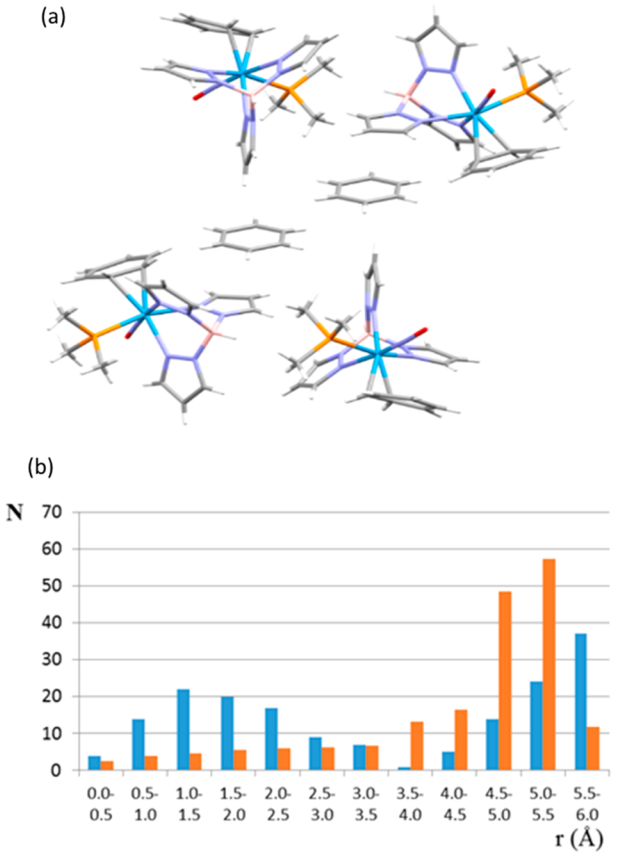

Figure 4. (a) Parallel benzene−benzene interaction with a large offset (r = 4.81 Å) in the crystal structure of EREYUV.[52] Both benzene molecules, involved in parallel interaction, also form CH/π and stacking interactions on both sides of the rings with molecules from the environment. (b) Histogram of the offset values r for phenyl−cyclohexyl[19] (blue, left bars) and benzene−benzene (orange, right bars)[30] interactions. N is the number of interactions.

interactions on both sides of benzene (CH/π and stacking) which is not possible in benzene stacking interactions with smaller offset values.

The specific behavior of the benzene−benzene interactions is illustrated by the benzene−benzene and benzene−cyclohexane interactions in crystal structures. The data in Figure 4b show quite different offset distributions for stacked benzene−benzene[30] and benzene−cyclohexane[19] in crystal structures. Specifically, most benzene−benzene interactions (orange, right bars, Figure 4b) were observed for large offsets, from 4.5 to 5.5 Å, with a very small number of the interactions at small offsets. Such a tendency is not so pronounced for phenyl−cyclohexyl contacts (blue, left bars, Figure 4b). Here again, this is due to benzene interactions at large offsets, since most of the maximum possible interaction energy is preserved at large offsets (Table 1, Figure 3). As was mentioned above, an additional advantage of non-negligible interactions at large offsets in supramolecular structures is the possibility of forming simultaneous interactions (Figure 4a).

The SAPT method[53] provides insight into the nature of the cyclohexane−benzene and benzene−benzene stacking interactions, including interactions at large horizontal displacements. We used a SAPT method with a density-fitting approximation (DF-SAPT2+3)[54] and the def2-tzvppd basis set, since using this basis set gave results in good agreement with accurate CCSD(T)/CBS energies (Tables 1 and 2, Tables S1−S6). The calculations were performed using the PSI4 program.[55] The data show that the most important contribution to the total energy is dispersion at all offsets for both systems (Tables 1 and 2). The second important attractive contribution is electrostatics, with the exception of the benzene−benzene sandwich geometry (r = 0.0 Å), where the electrostatic term is repulsive. If we add the attractive dispersion term to the exchange, the resulting net dispersion is less attractive than −1.0 kcal/mol, except for the benzene−benzene sandwich geometry.

In the cyclohexane−benzene dimer, the electrostatic term at small offsets (0.0 and 1.5 Å) is more attractive than the net dispersion, while at larger offsets (4.0 and 5.0 Å) the net dispersion term is more attractive than the electrostatic term. The benzene−benzene interaction is different: the net dispersion term dominates at the offset of 0.0 Å, while the electrostatic term dominates at other offsets and decreases only slightly with increasing offset.

These differences are illustrated in Figure 5 which shows the key energy terms as a function of the displacement (r) for both cyclohexane−benzene and benzene−benzene. Hence, the

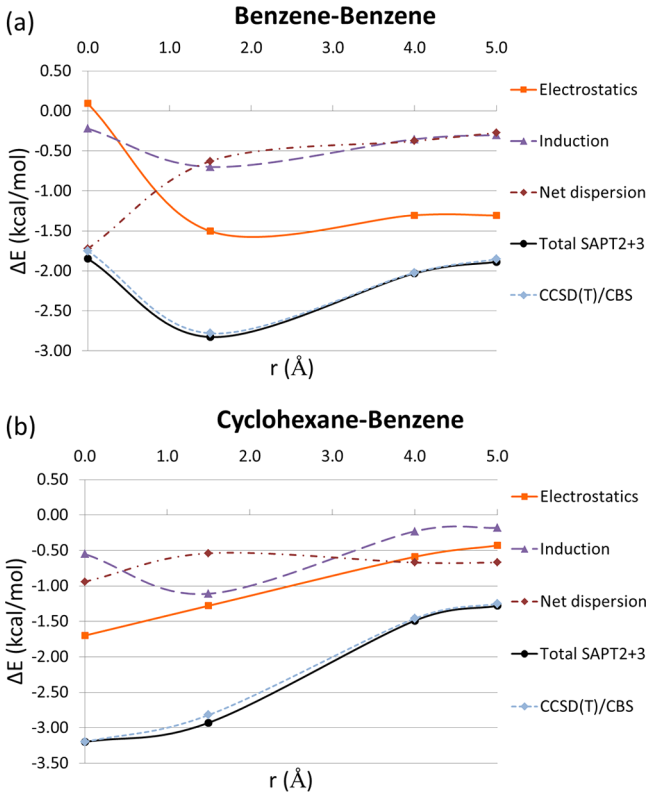

Figure 5. Results of SAPT analysis and CCSD(T)/CBS calculations for (a) benzene−benzene and (b) cyclohexane−benzene at several offset values. All interaction energies and selected energy components are average (Tables 1 and 2) and given in kcal/mol.

https://dx.doi.org/10.1021/acscentsci.0c00005
ACS Cent. Sci. 2020, 6, 420−425

significantly more attractive cyclohexane−benzene interaction, at 0.0 Å offset, is mostly a consequence of attractive electrostatic energy. At 1.5 Å offset electrostatics is the most dominant in both systems; it is still somewhat stronger in benzene−cyclohexane, causing slightly stronger interaction. At larger displacements the benzene−benzene interaction is stronger than the benzene−cyclohexane interaction, mostly due to more favorable electrostatic contribution in benzene−benzene dimer, despite the fact that net dispersion is slightly more favorable in cyclohexane−benzene than in benzene−benzene dimer.

The importance of the electrostatic term in benzene−benzene stacking interaction at small offsets is well-known.[56,57] The electrostatic term remains quite favorable at large offset in the benzene−benzene interaction because the local C−H dipoles are in an antiparallel orientation, as illustrated in Figure 6. On the other hand, in cyclohexane−benzene interaction the C−H dipoles are at right angles; hence, the electrostatic attraction is relatively small. One can also notice that hydrogen atoms in the cyclohexane molecule have significantly smaller positive potentials (Figure 6).

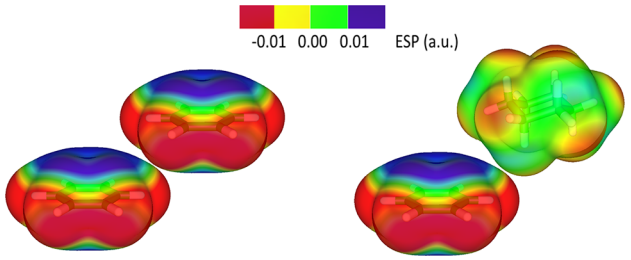

Figure 6. Overlaid electrostatic potentials for benzene−benzene and cyclohexane−benzene interactions at 5.0 Å. Electrostatic potentials for cyclohexane and benzene were plotted on a contour with an electron density of 0.001 e^{-}/(a.u.).[3]

CONCLUSIONS

Based on SAPT analysis one can conclude that the difference in potential energy surfaces for cyclohexane−benzene and benzene−benzene is a consequence of the ability of cyclohexane−benzene to form strong electrostatic interactions at small offset, and the capability of benzene−benzene to preserve relatively strong electrostatics at large offsets.

The potential curves in Figure 3 indicate that the important advantage of aromatic−aromatic interactions is the larger range of the attractive interactions (Figure 1), which arise from the long-range nature of the electrostatic interactions (Figure 5a). The stronger interaction at large offsets is the key feature that makes aromatic−aromatic interactions special. As illustrated in Figure 1, strong benzene−benzene attraction (>−2.0 kcal/mol) occurs up to ∼4.5 Å, which gives a 4.5 Å radius of attraction while that for cyclohexane−benzene is only 2.75 Å. After subtracting the small area where benzene−benzene interactions are weaker than −2.0 kcal/mol the area of strong attraction is 61.8 $Å^2$, while that for cyclohexane−benzene is only 23.8 $Å^2$ (Figure 1). Therefore, the "region of attraction" stronger than −2.0 kcal/mol is 2.5 times larger for benzene−benzene than for cyclohexane−benzene. Thus, benzene−benzene stacking interactions have a remarkable advantage since two benzenes (phenyl groups) can recognize each other over a much greater range of distances.

ASSOCIATED CONTENT

Supporting Information

The Supporting Information is available free of charge at https://pubs.acs.org/doi/10.1021/acscentsci.0c00005.

Additional calculations, data, and figures including structures and interaction energies (PDF)

AUTHOR INFORMATION

Corresponding Authors

Michael B. Hall − *Department of Chemistry, Texas A&M University, College Station, Texas 77843-3255, United States;* orcid.org/0000-0003-3263-3219; Email: hall@science.tamu.edu

Snežana D. Zarić − *Faculty of Chemistry, University of Belgrade, Belgrade 11000, Serbia; Department of Chemistry, Texas A&M University at Qatar, Doha, Qatar;* orcid.org/0000-0002-6067-2349; Email: szaric@chem.bg.ac.rs

Authors

Dragan B. Ninković − *Innovation Center of the Faculty of Chemistry in Belgrade, Belgrade 11001, Serbia*

Jelena P. Blagojević Filipović − *Innovation Center of the Faculty of Chemistry in Belgrade, Belgrade 11001, Serbia*

Edward N. Brothers − *Department of Chemistry, Texas A&M University at Qatar, Doha, Qatar*

Complete contact information is available at: https://pubs.acs.org/10.1021/acscentsci.0c00005

Notes

The authors declare no competing financial interest.

ACKNOWLEDGMENTS

This work was supported by the Serbian Ministry of Education, Science and Technological Development (Grant 172065). M.B.H. acknowledges support from the Welch Foundation, Grant A-0648, and the National Science Foundation, Grant CHE-1664866.

REFERENCES

(1) Tahara, K.; Fujita, T.; Sonoda, M.; Shiro, M.; Tobe, Y. Donors and Acceptors Based on Triangular Dehydrobenzo[12]annulenes: Formation of a Triple-Layered Rosette Structure by a Charge-Transfer Complex. *J. Am. Chem. Soc.* **2008**, *130*, 14339−14345.

(2) Fasan, R.; Dias, R. L. A.; Moehle, K.; Zerbe, O.; Obrecht, D.; Mittl, P. R. E.; Grütter, M. G.; Robinson, J. A. Structure-activity studies in a family of beta-hairpin protein epitope mimetic inhibitors of the p53-HDM2 protein-protein interaction. *ChemBioChem* **2006**, *7*, 515−526.

(3) Wheeler, S. E. Local Nature of Substituent Effects in Stacking Interactions. *J. Am. Chem. Soc.* **2011**, *133* (26), 10262−10274.

(4) Zhou, Y.; Li, B.; Li, S.; Ardoña, H. A. M.; Wilson, W. L.; Tovar, J. D.; Schroeder, C. M. Concentration-Driven Assembly and Sol−Gel Transition of π-Conjugated Oligopeptides. *ACS Cent. Sci.* **2017**, *3*, 986−994.

(5) Desiraju, G. R. Supramolecular synthons in crystal engineering - a new organic synthesis. *Angew. Chem., Int. Ed. Engl.* **1995**, *34*, 2311−2327.

(6) Fitchett, C. M.; Richardson, C.; Steel, P. J. Solid state conformations of symmetrical aromatic biheterocycles: an X-ray crystallographic investigation. *Org. Biomol. Chem.* **2005**, *3*, 498−502.

(7) Lukin, O.; Schubert, D.; Müller, C. M.; Schweizer, W. B.; Gramlich, V.; Schneider, J.; Dolgonos, G.; Shivanyuk, A. Engineering crystals of dendritic molecules. *Proc. Natl. Acad. Sci. U. S. A.* **2009**, *106*, 10922−10927.

(8) Varughese, S.; Pedireddi, V. R. A Competitive Molecular Recognition Study: Syntheses and Analysis of Supramolecular Assemblies of 3,5-Dihydroxybenzoic Acid and Its Bromo Derivative with Some N-Donor Compounds. *Chem. - Eur. J.* **2006**, *12*, 1597−1609.
(9) Meyer, E. A.; Castellano, R. K.; Diederich, F. Interactions with aromatic rings in chemical and biological recognition. *Angew. Chem., Int. Ed.* **2003**, *42*, 1210−1250.
(10) Abd Manan, T. S. B.; Khan, T.; Sivapalan, S.; Jusoh, V.; Sapari, N.; Sarwono, A.; Ramli, R. M.; Harimurti, S.; Beddu, S.; Sadon, S. N.; Kamal, N. L. M.; Malakahmad, A. Application of response surface methodology for the optimization of polycyclic aromatic hydrocarbons degradation from potable water using photo-Fenton oxidation process. *Sci. Total Environ.* **2019**, *665*, 196−212.
(11) Wheeler, S. E.; Bloom, J. W. G. Toward a More Complete Understanding of Noncovalent Interactions Involving Aromatic Rings. *J. Phys. Chem. A* **2014**, *118*, 6133−6147.
(12) Šponer, J.; Riley, K. E.; Hobza, P. Nature and magnitude of aromatic stacking of nucleic acid bases. *Phys. Chem. Chem. Phys.* **2008**, *10*, 2595−2610.
(13) Geronimo, I.; Singh, N. J.; Kim, K. S. Nature of anion-templated π+−π+ interactions. *Phys. Chem. Chem. Phys.* **2011**, *13*, 11841−11845.
(14) Butterfield, S. M.; Patel, P. R.; Waters, M. L. Contribution of Aromatic Interactions to α-Helix Stability. *J. Am. Chem. Soc.* **2002**, *124*, 9751−9755.
(15) Grimme, S. Do Special Noncovalent π−π Stacking Interactions Really Exist? *Angew. Chem., Int. Ed.* **2008**, *47*, 3430−3434.
(16) Blagojević, J. P.; Zarić, S. D. Stacking interactions of hydrogen-bridged rings − stronger than the stacking of benzene molecules. *Chem. Commun.* **2015**, *51*, 12989−12991.
(17) Bloom, J. W. G.; Wheeler, S. E. Taking the Aromaticity out of Aromatic Interactions. *Angew. Chem., Int. Ed.* **2011**, *50*, 7847−7849.
(18) Kim, K. S.; Karthikeyan, S.; Singh, N. J. How Different Are Aromatic π Interactions from Aliphatic π Interactions and Non-π Stacking Interactions? *J. Chem. Theory Comput.* **2011**, *7*, 3471−3477.
(19) Ninković, D. B.; Vojislavljević-Vasilev, D. Z.; Medaković, V. B.; Hall, M. B.; Brothers, E. N.; Zarić, S. D. Aliphatic−aromatic stacking interactions in cyclohexane−benzene are stronger than aromatic−aromatic interaction in the benzene dimer. *Phys. Chem. Chem. Phys.* **2016**, *18*, 25791−25795.
(20) Cabaleiro-Lago, E. M.; Rodriguez-Otero, J. σ-σ, σ-π, and π-π Stacking Interactions between Six-Membered Cyclic Systems. Dispersion Dominates and Electrostatics Commands. *Chemistry Select* **2017**, *2*, 5157−5166.
(21) Cabaleiro-Lago, E. M.; Rodriguez-Otero, J. On the Nature of σ−σ, σ−π, and π−π Stacking in Extended Systems. *ACS Omega* **2018**, *3*, 9348−9359.
(22) Schweizer, W. B.; Dunitz, J. D. Quantum Mechanical Calculations for Benzene Dimer Energies: Present Problems and Future Challenges. *J. Chem. Theory Comput.* **2006**, *2*, 288−291.
(23) Rezac, J.; Hobza, P. Benzene dimer: dynamic structure and thermodynamics derived from on-the-fly ab initio DFT-D molecular dynamic simulations. *J. Chem. Theory Comput.* **2008**, *4*, 1835−1840.
(24) Pitonak, M.; Neogrady, P.; Rezac, J.; Jurecka, P.; Urban, M.; Hobza, P. Benzene Dimer: High-Level Wave Function and Density Functional Theory Calculations. *J. Chem. Theory Comput.* **2008**, *4*, 1829−1834.
(25) Bludský, O.; Rubeš, M.; Soldán, P.; Nachtigall, P. Investigation of the benzene-dimer potential energy surface: DFT/CCSD(T) correction scheme. *J. Chem. Phys.* **2008**, *128*, 114102-1−114102-8.
(26) Janowski, T.; Pulay, P. High accuracy benchmark calculations on the benzene dimer potential energy surface. *Chem. Phys. Lett.* **2007**, *447*, 27−32.
(27) Bettinger, H. F.; Kar, T.; Sanchez-Garcia, E. Borazine and Benzene Homo- and Heterodimers. *J. Phys. Chem. A* **2009**, *113*, 3353−3359.
(28) Hohenstein, E. G.; Sherrill, C. D. Effects of Heteroatoms on Aromatic π−π Interactions: Benzene−Pyridine and Pyridine Dimer. *J. Phys. Chem. A* **2009**, *113* (5), 878−886.
(29) Lee, E. C.; Kim, D.; Jurečka, P.; Tarakeshwar, P.; Hobza, P.; Kim, K. S. Understanding of assembly phenomena by aromatic-aromatic interactions: benzene dimer and the substituted systems. *J. Phys. Chem. A* **2007**, *111*, 3446−3457.
(30) Ninković, D. B.; Janjić, G. V.; Veljković, D. Ž.; Sredojević, D. N.; Zarić, S. D. What are the preferred horizontal displacements in parallel aromatic-aromatic interactions? Significant interactions at large displacements. *ChemPhysChem* **2011**, *12*, 3511−3514.
(31) Ninković, D. B.; Andrić, J. M.; Malkov, S. N.; Zarić, S. D. What are the preferred horizontal displacements of aromatic−aromatic interactions in proteins? Comparison with the calculated benzene−benzene potential energy surface. *Phys. Chem. Chem. Phys.* **2014**, *16*, 11173−11177.
(32) Ninković, D. B.; Andrić, J. M.; Zarić, S. D. Parallel interactions at large horizontal displacement in pyridine-pyridine and benzene-pyridine dimers. *ChemPhysChem* **2013**, *14*, 237−243.
(33) Sinnokrot, M. O.; Valeev, E. F.; Sherrill, C. D. Estimates of the ab initio limit for pi-pi interactions: the benzene dimer. *J. Am. Chem. Soc.* **2002**, *124*, 10887−10893.
(34) Newberry, R. W.; Raines, R. T. Secondary Forces in Protein Folding. *ACS Chem. Biol.* **2019**, *14* (8), 1677−1686.
(35) Makwana, K. M.; Mahalakshmi, R. Implications of aromatic−aromatic interactions: From protein structures to peptide models. *Protein Sci.* **2015**, *24*, 1920−1933.
(36) Hong, H. Toward understanding driving forces in membrane protein folding. *Arch. Biochem. Biophys.* **2014**, *564*, 297−313.
(37) Riley, K. E.; Hobza, P. On the Importance and Origin of Aromatic Interactions in Chemistry and Biodisciplines. *Acc. Chem. Res.* **2013**, *46*, 927−936.
(38) Klosterman, J. K.; Yamauchia, Y.; Fujita, M. Engineering discrete stacks of aromatic molecules. *Chem. Soc. Rev.* **2009**, *38*, 1714−1725.
(39) Du, M.; Li, C.-P.; Zhao, X.-J.; Yu, Q. Interplay of coordinative and supramolecular interactions in engineering unusual crystalline architectures of low-dimensional metal−pamoate complexes under co-ligand intervention. *CrystEngComm* **2007**, *9*, 1011−1028.
(40) Khlobystov, A. N.; Blake, A. J.; Champness, N. R.; Lemenovskii, D. A.; Majouga, A. G.; Zyk, N. V.; Schröder, M. Supramolecular design of one-dimensional coordination polymers based on silver(I) complexes of aromatic nitrogen-donor ligands. *Coord. Chem. Rev.* **2001**, *222*, 155−192.
(41) Fujii, S.; Tada, T.; Komoto, Y.; Osuga, T.; Murase, T.; Fujita, M.; Kiguchi, M. Rectifying Electron-Transport Properties through Stacks of Aromatic Molecules Inserted into a Self-Assembled Cage. *J. Am. Chem. Soc.* **2015**, *137*, 5939−5947.
(42) Sutradhar, M.; Pombeiro, A. J. L. *Non-Covalent Interactions in the Synthesis and Design of New Compounds*; John Wiley & Sons, 2016; p 101.
(43) Mahmudov, K. T.; Gurbanov, A. V.; Guseinov, F. I.; Guedes da Silva, M. F. C. Noncovalent interactions in metal complex catalysis. *Coord. Chem. Rev.* **2019**, *387*, 32−46.
(44) Krenske, E. H.; Houk, K. N. Aromatic Interactions as Control Elements in Stereoselective Organic Reactions. *Acc. Chem. Res.* **2013**, *46*, 979−989.
(45) Hunter, C. A.; Lawson, K. R.; Perkins, J.; Urch, C. J. Aromatic interactions. *J. Chem. Soc. Perkin Trans. 2* **2001**, *5*, 651−669.
(46) Kolb, H. C.; Andersson, P. G.; Sharpless, K. B. Toward an Understanding of the High Enantioselectivity in the Osmium-Catalyzed Asymmetric Dihydroxylation (AD). 1. Kinetics. *J. Am. Chem. Soc.* **1994**, *116*, 1278−1291.
(47) Mollazadeh, S.; Sahebkar, A.; Hadizadeh, F.; Behravan, J.; Arabzadeh, S. Structural and functional aspects of P-glycoprotein and its inhibitors. *Life Sci.* **2018**, *214*, 118−123.
(48) Pappenberger, G.; Schulz-Gasch, T.; Kusznir, E.; Müller, F.; Hennig, M. Structure-assisted discovery of an aminothiazole derivative as a lead molecule for inhibition of bacterial fatty-acid

synthesis. *Acta Crystallogr., Sect. D: Biol. Crystallogr.* **2007**, *63*, 1208−1216.
(49) Steuber, H.; Heine, A.; Klebe, G. Applying thermodynamic profiling in lead finding and optimization. *J. Mol. Biol.* **2007**, *368*, 618−638.
(50) Mackie, I. D.; DiLabio, G. A. Approximations to complete basis set-extrapolated, highly correlated non-covalent interaction energies. *J. Chem. Phys.* **2011**, *135*, 134318.
(51) Frisch, M. J.; Trucks, G. W.; Schlegel, H. B.; Scuseria, G. E.; Robb, M. A.; Cheeseman, J. R.; Scalmani, G.; Barone, V.; Mennucci, B.; Petersson, G. A.; Nakatsuji, H.; Caricato, M.; Li, X.; Hratchian, H. P.; Izmaylov, A. F.; Bloino, J.; Zheng, G.; Sonnenberg, J. L.; Hada, M.; Ehara, M.; Toyota, K.; Fukuda, R.; Hasegawa, J.; Ishida, M.; Nakajima, T.; Honda, Y.; Kitao, O.; Nakai, H.; Vreven, T.; Montgomery, J. A., Jr.; Peralta, J. E.; Ogliaro, F.; Bearpark, M.; Heyd, J. J.; Brothers, E.; Kudin, K. N.; Staroverov, V. N.; Kobayashi, R.; Normand, J.; Raghavachari, K.; Rendell, A.; Burant, J. C.; Iyengar, S. S.; Tomasi, J.; Cossi, M.; Rega, N.; Millam, J. M.; Klene, M.; Knox, J. E.; Cross, J. B.; Bakken, V.; Adamo, C.; Jaramillo, J.; Gomperts, R.; Stratmann, R. E.; Yazyev, O.; Austin, A. J.; Cammi, R.; Pomelli, C.; Ochterski, J. W.; Martin, R. L.; Morokuma, K.; Zakrzewski, V. G.; Voth, G. A.; Salvador, P.; Dannenberg, J. J.; Dapprich, S.; Daniels, A. D.; Farkas, O.; Foresman, J. B.; Ortiz, J. V.; Cioslowski, J.; Fox, D. J. *Gaussian 09*, revision D.01; Gaussian, Inc.: Wallingford, CT, 2016.
(52) Graham, P. M.; Meiere, S. H.; Sabat, M.; Harman, W. D. Dearomatization of Benzene, Deamidization of N,N-Dimethylformamide, and a Versatile New Tungsten π Base. *Organometallics* **2003**, *22*, 4364−4366.
(53) Jeziorski, B.; Moszynski, R.; Szalewicz, K. Perturbation Theory Approach to Intermolecular Potential Energy Surfaces of van der Waals Complexes. *Chem. Rev.* **1994**, *94*, 1887−1930.
(54) Hohenstein, E. G.; Sherrill, C. D. Density fitting of intramonomer correlation effects in symmetry-adapted perturbation theory. *J. Chem. Phys.* **2010**, *133*, No. 014101.
(55) Turney, J. M.; Simmonett, A. C.; Parrish, R. M.; Hohenstein, E. G.; Evangelista, F.; Fermann, J. T.; Mintz, B. J.; Burns, L. A.; Wilke, J. J.; Abrams, M. L.; Russ, N. J.; Leininger, M. L.; Janssen, C. L.; Seidl, E. T.; Allen, W. D.; Schaefer, H. F.; King, R. A.; Valeev, E. F.; Sherrill, C. D.; Crawford, T. D. Psi4: An open-source ab initio electronic structure program. *WIREs Comput. Mol. Sci.* **2012**, *2*, 556.
(56) Hohenstein, E. G.; Duan, J.; Sherrill, C. D. Origin of the Surprising Enhancement of Electrostatic Energies by Electron-Donating Substituents in Substituted Sandwich Benzene Dimers. *J. Am. Chem. Soc.* **2011**, *133* (34), 13244−13247.
(57) Watt, M.; Hardebeck, L. K. E.; Kirkpatrick, C. C.; Lewis, M. Face-to-Face Arene−Arene Binding Energies: Dominated by Dispersion but Predicted by Electrostatic and Dispersion/Polarizability Substituent Constants. *J. Am. Chem. Soc.* **2011**, *133* (11), 3854−3862.

https://dx.doi.org/10.1021/acscentsci.0c00005
ACS Cent. Sci. 2020, 6, 420−425